Date of publication xxxx 00, 0000, date of current version xxxx 00, 0000.

Digital Object Identifier 10.1109/ACCESS.2017.Doi Number

Automatic Extrinsic Calibration of a Camera and a 2D LiDAR with Point-Line Correspondences

Jae-Yeul Kim[1] and Jong-Eun Ha[2]

[1]Graduate School of Information and Communication Engineering, Daegu Gyeongbuk Institute of Science & Technology (DGIST), Daegu 42988, South Korea

[2]Department of Mechanical and Automotive Engineering, Seoul National University of Science and Technology, Seoul 01811, South Korea

Corresponding author: Jong-Eun Ha (e-mail: jeha@ seoultech.ac.kr).

This study was supported by the Research Program funded by the SeoulTech (Seoul National University of Science and Technology).

ABSTRACT Extrinsic calibration of a 2D camera and a 2D LiDAR is necessary to fuse information from two sensors by representing the information under the same frame. Various geometric constraints such as point-plane, point-line, and point-point are used for the extrinsic calibration. Usually, these require a manual step, including control points selection for camera calibration and LiDAR points. We propose a new algorithm for automatic extrinsic calibration with point-line correspondences. A calibration structure with two perpendicular planes having a chessboard on both sides is used for the extrinsic calibration. First, we use predefined colors at specific locations on a chessboard to quickly find the origin of the coordinate system. Second, we robustly detect three control points on LiDAR raw data using a geometric constraint that two end points among three control points should lie on the same line. The initial linear solution is obtained by using a point-line constraint. Finally, it is refined by nonlinear minimization, which gives a 15.3% improvement compared to the linear solution. Experimental results show the feasibility of the proposed algorithm.

INDEX TERMS Extrinsic calibration, sensor fusion, camera, LiDAR

I. INTRODUCTION

The first necessary step is extrinsic calibration between a camera and a LiDAR to integrate information from them. LiDAR directly offers 3D information compared to the camera, which requires additional steps to provide depth information. Meanwhile, the camera offers more diverse and dense information about the scene. Sensor fusion aims to obtain more information than only using a single sensor.

This paper presents a method for the automatic extrinsic calibration of a camera and a LiDAR. We use a calibration structure consisting of two perpendicular planes. Chessboard patterns are used for the calibration of the camera. We use some distinct colors on a chessboard to easily identify the world frame on the chessboard. Conventional algorithms use black and white chessboard. We use a point-line constraint [5] for the extrinsic calibration of a camera and a LiDAR. We automatically detect control points from LiDAR data using a geometric constraint that a calibration structure lies on a plane. Also, we present a quantitative evaluation of the proposed method using a real trajectory of LiDAR. We use an additional camera having no infrared cut filter to find the real trajectory of LiDAR [30].

In our previous work [30], we presented an extrinsic calibration algorithm of a camera and a LiDAR, which uses the real trajectory of the LiDAR. In [30], we improved the performance of the Hu algorithm [12], which provides a linear solution using one shot with 3D-3D correspondences based on Perspective 3 Points (P3P) [31]. Our previous work [30] involves the manual selection of control points. In this paper, we propose an automatic algorithm for the extrinsic calibration of the camera and LiDAR. We propose to use a chessboard with distinct colors at predefined locations for camera calibration. Also, we automatically detect control points from LiDAR trajectories using a geometric constraint. Finally, we use multiple datasets acquired under different poses to improve the extrinsic calibration. We use a point-line constraint [5] for the automatic extrinsic calibration, while our previous work [30] used a constraint based on P3P.

The paper is organized as follows. Section II deals with related works. Section III shows the proposed method,

including automatic camera calibration and LiDAR control point detection. Experimental results are presented in section IV. Finally, the conclusion is in section V.

II. RELATED WORKS

Methods for the extrinsic calibration of LiDAR and camera can be categorized into target-based and targetless.

A. TARGET-BASED CALIBRATION

Wasielewski and Strauss [1] used a V-shaped calibration structure for the extrinsic calibration of multiple cameras and LiDARs. Zhang and Press [2] proposed an algorithm based on the constraint that LiDAR points should lie on a plane. Li et al. [3] proposed an algorithm that uses a triangular structure at right angles to each other. The solution is computed by a nonlinear minimization with constraints derived from points and straight lines after the manual designation of the initial solution. Kassir and Peynot [4] suggest an automated method by automating the entire process of related LiDAR data processing and camera calibration in the algorithm of Zhang and Press [2].

Bok et al. [5] proposed an algorithm that gives a linear solution using point-line constraints. Kwak et al. [6] used a V-shaped structure, and they used constraints between points and straight lines. Yang et al. [7] proposed an extrinsic calibration algorithm of a camera and a LiDAR using a Perspective-n-Point (PnP) method [8] by using the infrared filter to find a LiDAR trajectory on an image. Gomez-Ojeda et al. [9] used triangular structure perpendicular to each other, which is typical at the corner side in indoor environments. They used constraints derived from line-plane and point-plane.

Vasconcelos et al. [10] used a correspondence relationship between a plane and a straight line, giving a maximum of eight solutions. A linear solution based on the PnP-based method is presented. Zhou [11] proposed an extrinsic calibration method that uses correspondences among three planes and three straight lines. Hu et al. [12] proposed a possible algorithm using one shot with a PnP method using three mutually perpendicular planes. Li et al. [13] used a V-shape board with an adjustable angle between two planes and presented an analytical solution with a single observation.

Fan et al. [14] used a photogrammetric control field with even distribution of control points for the extrinsic calibration of a camera and a LiDAR. Briales and Gonzalez-Jimenez [15] proposed an algorithm using corners in an orthogonal trihedron structure. Zhu et al. [16] proposed an extrinsic calibration algorithm for multiple LiDARs using the corners of three perpendicular planes. Tian et al. [17] proposed a three-step algorithm using a checkerboard trihedron. Chen et al. [18] proposed an algorithm for automatic extrinsic calibration by aligning the geometric corners on a checkerboard. Fan et al. [19] proposed a two-stage algorithm for the extrinsic calibration of the camera and LiDAR with a specially designed calibration structure combining a sphere with a calibration plate.

B. TARGETLESS CALIBRATION

Targetless extrinsic calibration of camera and LiDAR usually uses scene information common for both sensors. They estimate extrinsic parameters by evaluating the consistency between LiDAR point clouds and camera images. Some approaches [20-22] first extract characteristic features like edge points from the camera and LiDAR and find extrinsic parameters by minimizing reprojection error between 2D-3D corresponding points. These approaches require that the target scene should include rich geometric features. Other approaches [23-26] reflect the different modalities of camera and LiDAR and use metrics based on mutual information.

Koide et al. [27] presented an open source for a fully automatic camera-LiDAR calibration toolbox that only uses one shot of the camera and LiDAR data without a calibration target. Sun et al. [28] proposed an extrinsic calibration algorithm that uses instance segmentation results of image and point cloud. They extracted and correlated key targets from the segmented instances. Chen et al. [29] proposed PBACalib for camera and LiDAR extrinsic calibration. They used plane-constrained bundle adjustment that uses feature points extracted from a prominent plane in the scene.

The proposed method belongs to the target-based calibration. We use a calibration structure consisting of two planes with a chessboard. The proposed algorithm uses distinct colors at predefined locations on the chessboard and uses a geometric constraint in extracting control points on LiDAR data to automate the extrinsic calibration.

III. PROPOSED METHOD

Figure 1 shows the flow chart of the proposed method and system' configuration. It consists of two cameras and one LiDAR. The dummy camera with the infrared cut-off filter removed is used for quantitative evaluation of extrinsic calibration because it can detect the actual trajectory of LiDAR. Our previous work [30] proposed an extrinsic calibration algorithm using a dummy camera with an IR cut filter removed. In [30], we manually extracted control points on an image from a dummy camera and used them for extrinsic calibration. This paper deals with automatic extrinsic calibration between a camera and a 2D LiDAR. We use a dummy camera that can observe the actual trajectories of LiDAR for evaluation.

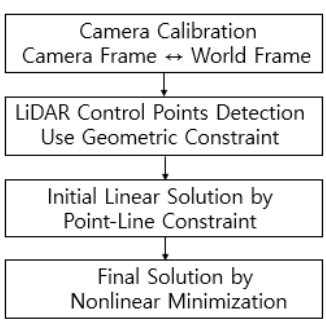

(a)

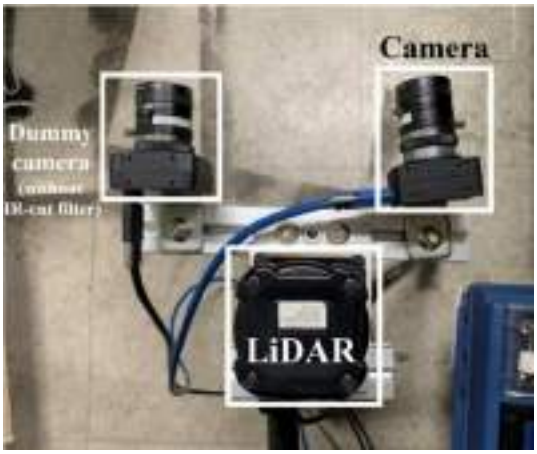

(b)

FIGURE 1. The schematic of the proposed method (a) flow chart of the proposed method. (b) system configuration.

A. AUTOMATIC EXTRINSIC CALIBRATION BETWEEN WORLD AND CAMERA FRAME

The extrinsic calibration between the camera and the world coordinate system must be done before extrinsic calibration between the camera and LiDAR. Automatic chessboard detection and arrangement of coordinates corresponding to each control point in the world coordinate system is required. We use different colors to ease the problem of assigning world coordinates on the chessboard, as shown in Figure 2. Figure 2 shows the calibration structure consisting of two planes.

We sequentially detect control points on two chessboard patterns in Figure 2. Figure 3 shows the intermediate results according to the proposed procedure. First, we detect all control points on one chessboard, as shown in Figure 3(a). Then we mask image regions corresponding to the detected chessboard, as shown in Figure 3(b). Finally, we detect control points on the second plane, as shown in Figure 3(c). We use all control points on two planes to improve the quality of the extrinsic calibration. Figure 4 shows all control points detected on two planes.

After detecting control points on two planes, it is necessary to represent them under the world coordinate system. We use different colors along each axis of a chessboard pattern to ease the identification of the world coordinate system. We use red, green, and blue as the reference for the axis, as shown in Figure 4.

A total of 36 control points are extracted from each plane. The 15th, 16th, 21st, and 22nd indices represent the vertices of the middle rectangle regardless of the rotation of a plane. We use different colors at this position to differentiate whether the current plane is left or right. We use red and blue as the center rectangle of each plane, as shown in Figure 4. Among 36 control points, points of the index (1, 6, 31, 36) correspond to the outermost points. We assign different colors to these extreme points, as shown in Figure 5, to quickly identify the origin of the coordinate system.

FIGURE 2. Calibration structure with two planes.

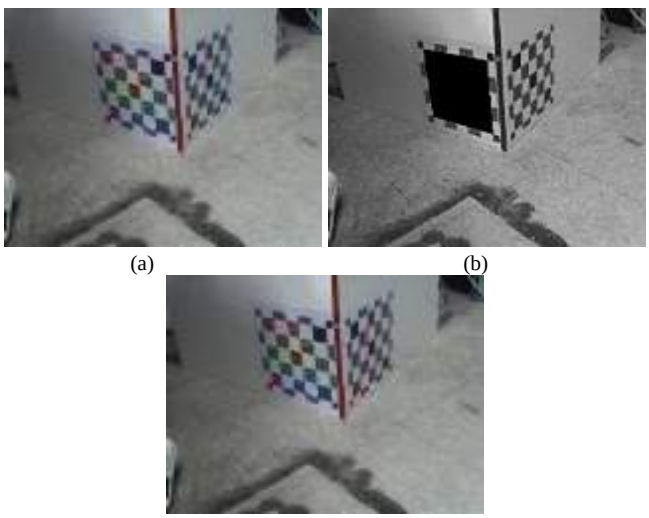

(a) (b)

(c)

FIGURE 3. Procedure of automatic detection of control points on the chessboard (a) first detection on a plane (b) automated masking detected plane (c) final detection on a second plane.

FIGURE 4. Automatically detected control points on the chessboard.

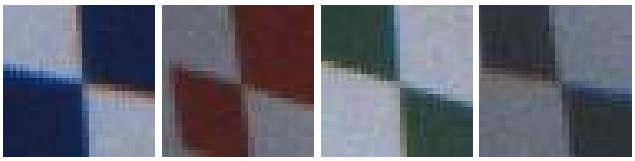

FIGURE 5. **Extraction of four control points on the chessboard's boundary.**

B. AUTOMATIC DETECTION OF LIDAR CONTROL POINTS

In this section, we deal with the automatic detection of control points in LiDAR data which is used for the extrinsic calibration of the camera and LiDAR. We use the same calibration structure in Figure 2, which is used for camera calibration. This section aims to find three control points on LiDAR data that lie on the three axes of the world frame, as shown in Figure 9.

We use the HOKUYO UTM-30LX LiDAR in experiments, and it provides coordinates for 1080 indices in the range of -135° to 135° covering 270°. Figure 6 shows the plot of the original LiDAR data. In Figure 6, the red rectangle corresponds to the calibration structure of two planes.

We automatically find the region corresponding to the red rectangle by searching 360 indices of -45° and 45°. As shown in Figure 7, we compute an angle for each point of 360 indices. We obtain two lines by fitting them using 10 points compared to the current point. In Figure 7, the left vector is the unit vector obtained by points after the current point, whereas the right vector is the unit vector obtained by points before the current point. Finally, the angle between two lines is computed, and we note it as θ, as shown in Figure 7.

Figure 8 shows the computed angle along 360 points. When a noticeable geometric change is near the projected point, θ will have a considerable value. Since the corner portion of the calibration structure in Figure 2 causes significant geometric change, θ value will have an enormous value in the corresponding index. The computation of θ uses 20 control points, 10 points each on the left and right, in the angle calculation. We use 10 points for line fitting, which is a large number of points for line fitting, to overcome noisy measurements of raw LiDAR data. Contrarily, the computed angle has a high value at the corner and surrounding points at the corner. If we apply a threshold, we have multiple candidate points for a control point. We find a point corresponding to the center of the connected 1D cluster after threshold.

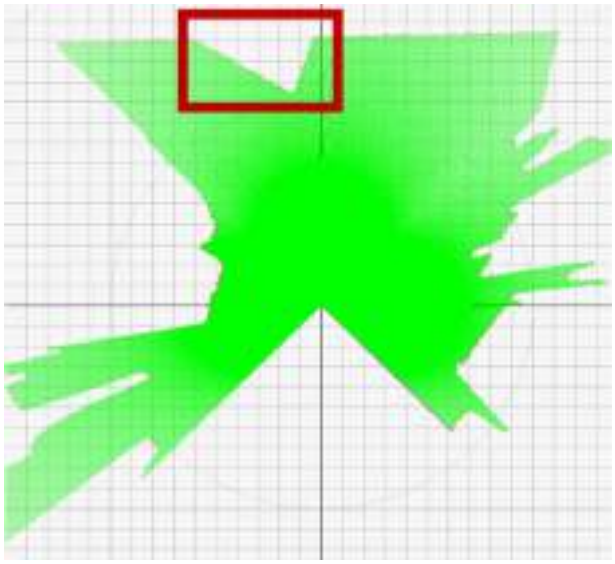

FIGURE 6. **Display of the whole LiDAR data (Red rectangle indicates the location of calibration structure).**

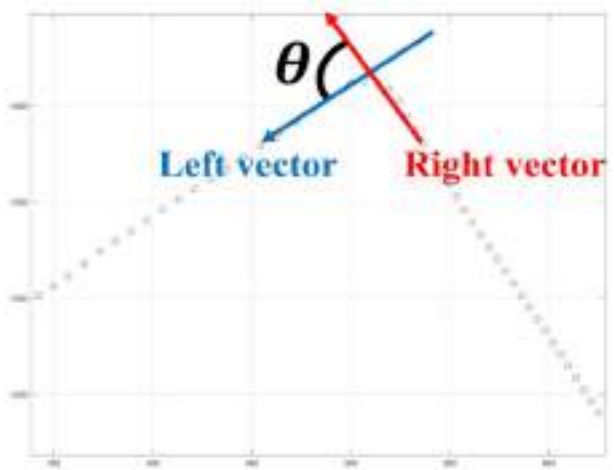

FIGURE 7. **The computation of an angle at the candidate control point.**

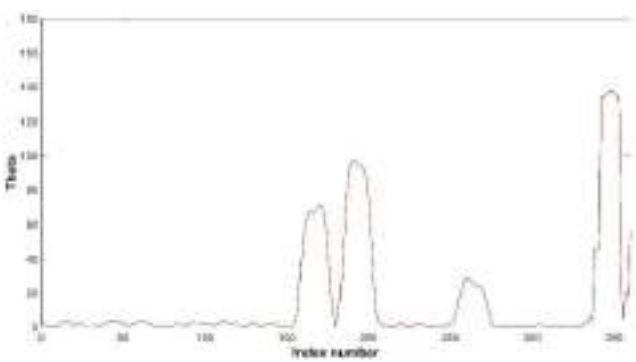

FIGURE 8. **The computed angle along the point index.**

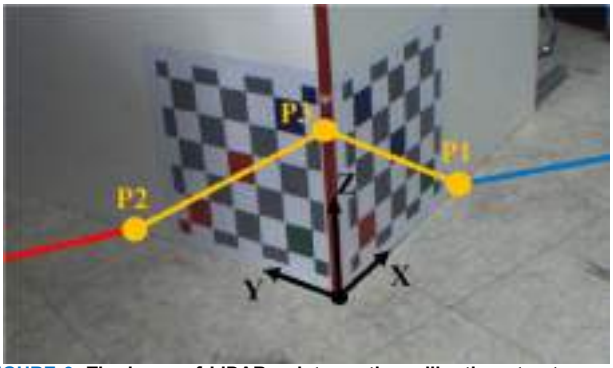

FIGURE 9. The locus of LiDAR points on the calibration structure and three control points on the world frame's each axis.

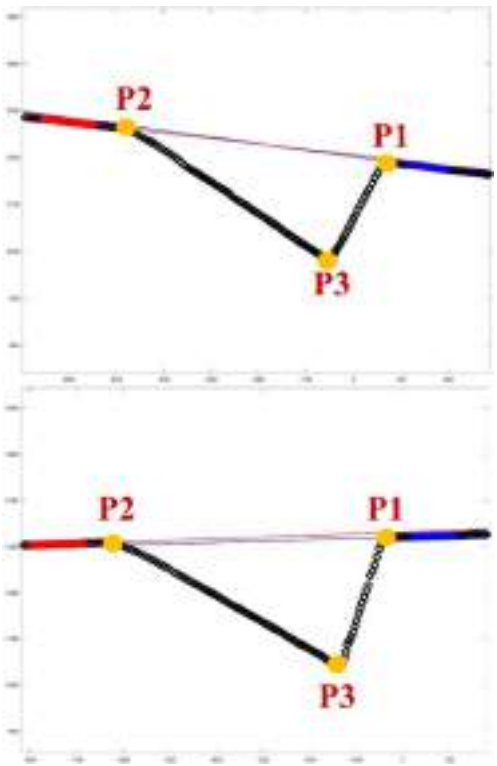

FIGURE 10. The line correspondence evaluation using the left and right parts of the calibration structure.

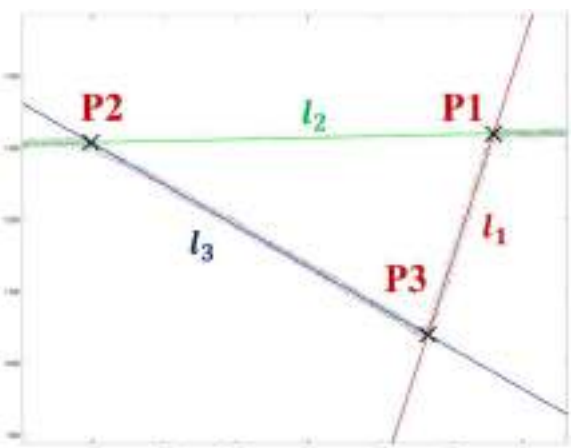

FIGURE 11. The computation of the line with regression and control points by finding the crossing point of two lines.

Throughout this step, we obtain multiple candidate points larger than three. The final goal is to select three control points in Figure 9. For this, we use an additional constraint. We use the fact that the calibration structure lies on a plane. Therefore, if we fit two lines each using red points and blue points in Figure 9, the two lines should be equal. In reality, the fitted two lines would show a slight difference, as shown in Figure 10, due to noise in the measurement. Finally, we choose (P1, P3, and P2) if the two lines are similar within the threshold. Figure 10 shows two cases of fitting two lines acquired under different poses. The proposed algorithm finds well three control points.

Further, we refine three points, P1, P2, and P3, using line fitting. In experiments, we show the effectiveness of the refinement of control points. Figure 11 shows the process involving line fitting. We fit a line l_1 using points in P1 and P3. We fit a line l_2 using points before P1 and points after P2. We fit a line l_3 using points in P2 and P3. We find a cross point of two lines, l_1 and l_2 and consider it as a refined point of P1. The same processing is done for lines l_2 and l_3 and for lines l_1 and l_3. Finally, we obtain refined three control points which gives a better extrinsic calibration.

C. COMPUTATION OF LINEAR SOLUTION

The proposed automatic extrinsic calibration algorithm of a camera and a 2D LiDAR consists of two steps. We first compute a linear solution using a point-line constraint [5]. Then, nonlinear minimization is applied to improve the linear solution.

In this section, we briefly review the point-line constraint [5]. The conversion between the camera and LiDAR coordinate systems is as follows.

$$\begin{bmatrix} x_c \\ y_c \\ z_c \end{bmatrix} = \begin{bmatrix} r_{11} & r_{12} & r_{13} \\ r_{21} & r_{22} & r_{23} \\ r_{31} & r_{32} & r_{33} \end{bmatrix} \begin{bmatrix} x_l \\ y_l \\ 0 \end{bmatrix} + \begin{bmatrix} t_x \\ t_y \\ t_z \end{bmatrix} \tag{1}$$

$(x_c,\ y_c,\ z_c)^T$ and $(x_l,\ y_l,\ z_l)^T$ represents a point under camera and LiDAR frame. $r_{ij}\ (i,j = 1,2,3)$ represents elements of 3X3 rotation matrix and $(t_x, t_y, t_z)^T$ is the translation vector between the camera and LiDAR frame. We use a 2D LiDAR therefore the point of LiDAR has the form of $(x_l,\ y_l,\ 0)^T$. Eq. (1) can be arranged as follows.

$$\begin{cases} x_c = r_{11}x_l + r_{12}y_l + t_x \\ y_c = r_{21}x_l + r_{22}y_l + t_y \\ z_c = r_{31}x_l + r_{32}y_l + t_z \end{cases} \tag{2}$$

A line in 3D under the camera frame can be represented as follows.

$$\frac{x-x_0}{l} = \frac{y-y_0}{m} = \frac{z-z_0}{n} \tag{3}$$

$(l, m, n)^T$ is a direction vector of the line. $(x_0,\ y_0,\ z_0)^T$is a point on the line. Eq. (3) can be represented into two

equations.

$$\frac{x-x_0}{l} = \frac{y-y_0}{m} \quad (4)$$

$$\frac{y-y_0}{m} = \frac{z-z_0}{n} \quad (5)$$

If a point under the camera frame lies on a line, it should satisfy the Eq. (4) and Eq. (5). If we insert Eq. (2) into Eq. (4) and Eq. (5), we can have the following.

$$\frac{r_{11}x_l+r_{12}y_l+t_x-x_0}{l} = \frac{r_{21}x_l+r_{22}y_l+t_y-y_0}{m} \quad (6)$$

$$\frac{r_{21}x_l+r_{22}y_l+t_y-y_0}{m} = \frac{r_{31}x_l+r_{32}y_l+t_z-z_0}{n} \quad (7)$$

Eq. (6) and Eq. (7) can be represented as follows.

$$\begin{bmatrix} mx_l & my_l - lx_l & -ly_l & 0 & 0 & m & -l & 0 \\ 0 & 0 & nx_l & ny_l - mx_l & -my_l & 0 & n & -m \end{bmatrix} \begin{bmatrix} r_{11} \\ r_{12} \\ r_{21} \\ r_{22} \\ r_{31} \\ r_{32} \\ t_x \\ t_y \\ t_z \end{bmatrix} = \begin{bmatrix} mx_0 - ly_0 \\ ny_0 - mz_0 \end{bmatrix} \quad (8)$$

One pair of point-line gives two constraints as Eq. (8). Therefore, if we have more than five pairs of point-line correspondences, we could have a linear solution using Eq. (8).

D. FINDING A SOLUTION USING NONLINEAR MINIMIZATION

We apply nonlinear minimization to improve the solution using a linear solution as the initial solution. For nonlinear minimization, the average distance of point-line correspondence pairs in the world frame used is used as cost. The cost term is defined as follows.

$$\mathrm{L} = \sum_{i=1}^{N} \sum_{j=1}^{3} d_{ij}\left(p_{ij}, l_{ij}\right) \quad (9)$$

$d(p, l)$ represents a distance between a point p and a line l in 3D Euclidean space. Index i is related to the dataset, and index j is related to control points in the i-th dataset. We use three control points for each dataset. Nonlinear minimization is done using an algorithm similar to MATLAB's fmincon function.

In the point-line correspondence pair used for extrinsic calibration, LiDAR control points P1, P2, and P3 are located on the world frame's X, Y, and Z axis, as shown in Figure 9. P1, P2, and P3 under the LiDAR frame are converted into a world frame, denoted as Q1, Q2, and Q3. The distances between Q1, Q2, and Q3 and the X-axis, Y-axis, and Z-axis are computed and used as cost. We use five sets for extrinsic calibration. We extract three control points from each set. Therefore 15 control points are used in the nonlinear minimization.

IV. EXPERIMENTAL RESULTS

The evaluation of extrinsic calibration is done using a separate dummy camera that can observe the actual trajectory of LiDAR by removing the infrared filter [30]. If we remove the infrared filter from the camera, we can detect the actual point the lidar is projecting. This enables a more accurate evaluation of extrinsic calibration.

We evaluate the accuracy of extrinsic calibration with the validation set acquired by a dummy camera. The calibration structure of Figure 2 is located at a predefined distance of seven locations at 0.5m, 1m, 1.5m, 2m, 3m, 4m, and 5m. Then we acquire three images per location by varying the location of the calibration structure on the image. For each image, we find one true location of actual LiDAR and use it for evaluation.

Figure 12 shows three images acquired at a predefine distance, and the green point corresponds to one selected ground-truth LiDAR point for evaluation. We additionally used a reflective tape to find a projected point of the LiDAR at a long distance. We use the upper part of the calibration structure for verification by attaching a chessboard pattern, as shown in Figure 12. Also, extrinsic calibration between the world and the camera frame is possible using the upper chessboard.

Figure 12 shows ground-truth control points for each image. We use one LiDAR point on the cross line of two planes for evaluation. We convert the control point under the camera frame into a world frame using extrinsic parameters between LiDAR and a dummy camera. We consider the Z coordinate of each control under the world frame as a ground-truth one, as shown in Table 3.

The evaluation of extrinsic calibration with ground-truth control point is done as follows. The location of the control point for evaluation is found in LiDAR data. Then the coordinate under the LiDAR frame is transformed into the coordinate under the camera frame using computed extrinsic parameters between LiDAR and the camera. Finally, it is converted into coordinates in a world frame using extrinsic parameters between the camera and the world frame. We compute the 3D Euclidean distance between the ground truth and the converted one and consider it an error.

We use five sets acquired by varying poses between the calibration structure and camera for the automatic extrinsic calibration of the camera and LiDAR. For each data, we extract three control points from the LiDAR trajectory. In total, 15 control points from five sets are used as point-line constraints for the automatic extrinsic calibration.

Table 1 shows computed extrinsic parameters by the proposed algorithm. Evaluation using the dummy camera is also presented. We notice that the nonlinear solution gives an improved result compared to the linear solution by comparing validation errors.

FIGURE 12. The dataset for evaluating extrinsic calibration (The green point is the ground truth).

TABLE 1 Result of automatic extrinsic calibration using control points by line regression.

	Computed R $(\theta_x\ \theta_y\ \theta_z)$ [deg]	Computed T $(t_x\ t_y\ t_z)$ [mm]	Validation Error [mm]
Linear solution	(-86.63, -0.53, 0.26)	(81.04, -49.04, -80.16)	40.36
Nonlinear solution	(-86.60, -0.46, 0.61)	(73.97, -49.01, -71.86)	34.20

In this paper, when performing external correction, the lidar control points P1, P2, and P3 are calculated using linear regression instead of the lidar's raw data. As shown in Figure 12 below, there is a difference of 10 mm between the coordinates calculated through linear regression and the raw data.

Table 2 shows the external correction results when using LIDAR data as it is without using linear regression. It can be seen that the projection accuracy is lower than that of Table 1. Therefore, when performing external calibration, it can be seen that higher results can be obtained if the coordinates of the control points are calculated through linear regression without using raw data.

The extrinsic calibration results are quantitatively evaluated in the 3D world frame. Also, we present the result by projecting the LiDAR point onto the image for qualitative evaluation, as shown in Figure 14. In Figure 14, the green circle represents the ground-truth point, and the red cross is the projected point. It can be seen that the final RT, which has undergone nonlinear minimization for various distances, shows an accurate projection.

Table 3 shows the comparison result of the ground truth world point and computed one by nonlinear minimization. We obtained three datasets at a fixed distance. A total of 21 points from seven locations are used in the evaluation.

Table 4 shows the error according to the distance of the evaluation set. We can notice that error increases as the distance get large. In all distances, the nonlinear solution gives improved results compared to the linear solution.

Table 5 compares the proposed method's result to our previous method [30]. Our previous method [30] requires a manual selection of control points. Therefore, the whole procedure is not automatic. Also, it used a constraint of the Hu algorithm [12], while the proposed method uses a point-line constraint. The proposed method gives a smaller error though the standard deviation is higher than our previous method [30]. Also, the proposed method can automate the whole procedure of extrinsic calibration.

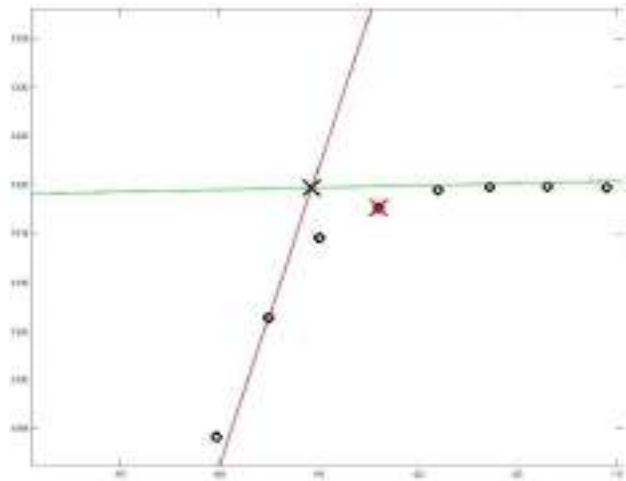

FIGURE 13. Comparison of control points obtained by line fitting and from raw data (the black cross shows the control point obtained by line fitting, and the red cross indicates the control point from raw data).

TABLE 2. Result of automatic extrinsic calibration using control points from raw data.

	Computed R $(\theta_x\ \theta_y\ \theta_z)$ [deg]	Computed T $(t_x\ t_y\ t_z)$ [mm]	Validation Error [mm]
Linear solution	(-86.75, -0.10, 0.91)	(43.56, -40.57, -76.75)	42.80
Nonlinear solution	(-86.73, -0.78, 1.23)	(58.59, -41.73, -74.00)	40.78

FIGURE 14. Projection results with computed extrinsic calibration on validation sets(green circle is the ground truth, and red cross is the projected point at distances of 0.5m, 1m, 1.5m, 2m, 3m, 4m, 5m).

TABLE 3. Comparison of computed world point by nonlinear solution.

Distance (Location)	Ground-truth (X, Y, Z) [mm]	Back-projected (X, Y, Z) [mm]	Error [mm]
0.5m (L)	(0, 0, 665.6)	(14.5, 4.7, 669.4)	15.7
0.5m (M)	(0, 0, 658.6)	(6.4, 4.2, 660.9)	8.0
0.5m (R)	(0, 0, 654.9)	(5.2, 6.7, 657.2)	8.8
1m (L)	(0, 0, 582.3)	(-7.7, -9.5, 585.4)	12.6
1m (M)	(0, 0, 574.7)	(-7.2, -8.1, 576.9)	11.1
1m (R)	(0, 0, 568.3)	(-10.6, -8.8, 570.4)	13.9
1.5m (L)	(0, 0, 646.6)	(-13.1, -13.6, 650.1)	19.2
1.5m (M)	(0, 0, 622.2)	(-10.6, -14.6, 624.9)	18.2
1.5m (R)	(0, 0, 605.5)	(-7.9, -15.9, 608.7)	18.0
2m (L)	(0, 0, 661.4)	(-21.3, -25.0, 666.2)	33.2
2m (M)	(0, 0, 643.8)	(-13.3, -22.8, 647.2)	26.6
2m (R)	(0, 0, 599.7)	(-10.6, -30.3, 601.8)	32.2
3m (L)	(0, 0, 670.9)	(-39.9, -38.8, 680.4)	56.5
3m (M)	(0, 0, 630.9)	(-30.8, -46.0, 636.4)	55.6
3m (R)	(0, 0, 596.4)	(-19.8, -54.0, 601.0)	57.7
4m (L)	(0, 0, 716.3)	(-36.8, -26.2, 734.9)	48.9
4m (M)	(0, 0, 656.9)	(-21.0, -40.4, 665.9)	46.4
4m (R)	(0, 0, 618.9)	(9.4, -45.9, 630.0)	48.2
5m (L)	(0, 0, 665.6)	(-44.5, -26.9, 686.0)	55.5
5m (M)	(0, 0, 708.0)	(-19.0, -57.5, 719.4)	61.6
5m (R)	(0, 0, 536.8)	(-0.59, -69.0, 550.9)	70.4

TABLE 4. The error of extrinsic calibration according to the distance.

	Error at distance (0.5m, 1.0m, 1.5m, 2m, 3m, 4m, 5m) [mm]	Mean Error [mm]
Linear solution	(4, 21, 27, 34, 66, 55, 70)	40.36
Nonlinear solution	(11, 13, 18, 31, 57, 48, 63)	34.20

TABLE 5. The comparison of the proposed method with our previous method [30].

	3D error [mm]
Our previous method [30]	46.34 ± 10.79
Proposed method	34.43 ± 21.60

V. CONCLUSION

This paper proposes a method for the automatic extrinsic calibration of LiDAR and a camera. The calibration structure consisted of two planes with a chessboard is used. We use predefined colors at predefined positions on the chessboard to easily identify the world frame on the calibration structure under diverse poses. Control points from LiDAR data are automatically detected using a geometric constraint. A linear solution is obtained using a point-line constraint. Finally, nonlinear minimization improves the linear solution using datasets acquired under different poses. The accuracy of the extrinsic calibration was evaluated using a dummy camera removing the IR cut filter, which provides a real trajectory of LiDAR. We can conclude that nonlinear minimization gives an improved solution than a linear solution through quantitative evaluation.

REFERENCES

[1] S. Wasielewski and O. Strauss, ``Calibration of a multi-sensor system laser range finder/camera," in Proc. Intell. Vehicles Symp., Sep. 1995, pp. 472-477.

[2] Q. Zhang and R. Pless, ``Extrinsic calibration of a camera and laser range finder (improves camera calibration)," in Proc. IEEE/RSJ Int. Conf. Intell. Robots Syst. (IROS), Sep./Oct. 2004, pp. 2301-2306.

[3] G. Li, Y. Liu, L. Dong, X. Cai, and D. Zhou, ``An algorithm for extrinsic parameters calibration of a camera and a laser range _nder using line features," in Proc. IEEE/RSJ Int. Conf. Intell. Robots Syst., Oct. 2007, pp. 3854-3859.

[4] A. Kassir and T. Peynot, ``Reliable automatic camera-laser calibration," in Proc. Australas. Conf. Robot. Automat., 2010, pp. 1-10.

[5] Y. S. Bok, Y. K. Jeong, D. G. Choi, and I. S. Kweon, ``Capturing village level heritages with a hand-held camera-laser sensor," Int. J. Comput. Vis., vol. 94, no. 1, pp. 36-53, 2011.

[6] K. Kwak, D. F. Huber, H. Badino, and T. Kanade, ``Extrinsic calibration of a single line scanning lidar and a camera," in Proc. IEEE/RSJ Int. Conf. Intell. Robots Syst., Sep. 2011, pp. 3283-3289.

[7] H. Yang, X. Liu, and I. Patras, ``A simple and effective extrinsic calibration method of a camera and a single line scanning LiDAR," in Proc. Int. Conf. Pattern Recognit., Nov. 2012, pp. 1439-1442.

[8] L. Quan and Z. Lan, ``Linear N-point camera pose determination," IEEE Trans. Pattern Anal. Mach. Intell., vol. 21, no. 8, pp. 774-780, Aug. 1999.

[9] R. Gomez-Ojeda, J. Briales, E. Fernandez-Moral, and J. Gonzalez-Jimenez, ``Extrinsic calibration of a 2D laser-range finder and a camera based on scene corners," in Proc. IEEE Int. Conf. Robot. Autom. (ICRA), May 2015, pp. 3611-3616.

[10] F. Vasconcelos, J. P. Barreto, and U. Nunes, ``A minimal solution for the extrinsic calibration of a camera and a laser-range finder," IEEE Trans. Pattern Anal. Mach. Intell., vol. 34, no. 11, pp. 2097-2107, Nov. 2012.

[11] L. Zhou, ``A new minimal solution for the extrinsic calibration of a 2D LIDAR and a camera using three plane-line correspondences," IEEE Sensors J., vol. 14, no. 2, pp. 442-454, Feb. 2014.

[12] Z. Hu, Y. Li, N. Li, and B. Zhao, ``Extrinsic calibration of 2-D laser range finder and camera from single shot based on minimal solution," IEEE Trans. Instrum. Meas., vol. 65, no. 4, pp. 915-929, Apr. 2016.

[13] N. Li, Z. Hu, and B. Zhao, ``Flexible extrinsic calibration of a camera and a two-dimensional laser range finder with a folding pattern," Appl. Opt., vol. 55, no. 9, pp. 2270-2280, 2016.

[14] J. Fan, Y. Huang, J. Shan, S. Zhang, and F. Zhu, ``Extrinsic calibration between a camera and a 2D laser range finder using a photogrammetric control field," Sensors, vol. 19, no. 9, p. 2030, Apr. 2019.

[15] J. Briales and J. Gonzalez-Jimenez, ``A minimal solution for the calibration of a 2D laser-range finder and a camera based on scene corners," in Proc. IEEE/RSJ Int. Conf. Intell. Robots Syst. (IROS), Sep. 2015, pp. 1891_1896.

[16] F. Zhu, Y. Huang, Z. Tian, and Y. Ma, ``Extrinsic calibration of multiple two-dimensional laser range finders based on a trihedron," Sensors, vol. 20, no. 7, p. 1837, Mar. 2020.
[17] Z. Tian, Y. Huang, F. Zhu, and Y. Ma, ``The extrinsic calibration of area-scan camera and 2D laser range finder (LRF) using checkerboard trihedron," IEEE Access, vol. 8, pp. 36166-36179, 2020.
[18] F. Chen, S. Zhang, X. Xie, Q. Zhang, Y. Wang, J. Jiao, and M. Liu, "Automatic multi-camera multi-LiDAR extrinsic calibration using geometric corners," IEEE 25th International Conference on Intelligent Transportation Systems (ITSC), Oct. 2022, pp. 4234-4240.
[19] S. Fan, Y. Yu, M. Xu, and L. Zhao, "High-precision external parameter calibration method for camera and lidar based on a calibration device," IEEE Access, vol. 11, pp. 18750-18760, 2023.
[20] C. Yuan, X. Liu, X. Hong, and F. Zhang, "Pixel-level extrinsic self-calibration of high resolution LiDAR and camera in targetless environments," IEEE Robotics and Automation Letters, vol. 6, no. 4, pp. 7517–7524, Oct. 2021.
[21] X. Zhang, S. Zhu, S. Guo, J. Li, and H. Liu, "Line-based automatic extrinsic calibration of LiDAR and camera," in IEEE International Conference on Robotics and Automation. IEEE, May 2021, pp. 9347-9353.
[22] X. Liu, C. Yuan, and F. Zhang, "Targetless extrinsic calibration of multiple small FoV LiDARs and cameras using adaptive voxelization," IEEE Transactions on Instrumentation and Measurement, vol. 71, pp. 1-12, May 2022.
[23] G. Pandey, J. McBride, S. Savarese, and R. Eustice, "Automatic targetless extrinsic calibration of a 3d lidar and camera by maximizing mutual information," AAAI Conference on Artificial Intelligence, vol. 26, no. 1, pp. 2053–2059, Sept. 2021.
[24] G. Pandey, J. R. McBride, S. Savarese, and R. M. Eustice, "Automatic extrinsic calibration of vision and lidar by maximizing mutual information," Journal of Field Robotics, vol. 32, no. 5, pp. 696–722, Sept. 2014.
[25] A. Stewart, "Localisation using the appearance of prior structure," Ph.D. dissertation, Oxford University, UK, 2016.
[26] J. Jeong, Y. Cho, and A. Kim, "The road is enough! Extrinsic calibration of non-overlapping stereo camera and LiDAR using road information," IEEE Robotics and Automation Letters, vol. 4, no. 3, pp. 2831–2838, July 2019.
[27] K. Koide, S. Oishi, M. Yokozuka, and A. Banno, "General, single-shot, target-less, and automatic LiDAR-camera extrinsic calibration toolbox," arXiv: 2302.05094, 2023.
[28] C. Sun, Z. Wei, W. Huang, Q. Liu, and B. Wang, "Automatic targetless calibration for LiDAR and camera based on instance segmentation," IEEE Robotics and Automation Letters, vol. 8, no. 2, pp. 981-988, 2023.
[29] F. Chen, L. Li, S. Zhang, J. Wu, and L. Wang, "PBACalib: Targetless extrinsic calibration for high-resolution LiDAR-camera system based on plane-constrained bundle adjustment," IEEE Robotics and Automation Letters, vol. 8, no. 1, pp. 304-311, 2023.
[30] J.-Y. Kim and J.-E. Ha, "Extrinsic calibration of a camera and a 2D LiDAR using a dummy camera with IR cut filter removed," IEEE Access, vol. 8, pp. 183071-183079, 2020.
[31] D. W. Eggert, A. Lorusso, and R. B. Fisher, ``Estimating 3-D rigid body transformations: A comparison of four major algorithms," *Mach. Vis. Appl.*, vol. 9, nos. 5-6, pp. 272-290, Mar. 1997.

JAE-YEUL KIM received his B.S. and M.E. degrees in mechanical and automotive engineering from the Graduate School of Automotive Engineering, Seoul National University of Science and Technology, Seoul, South Korea, in 2018 and 2021. He is pursuing a Ph.D. in information and communication engineering with the Graduate School, Daegu Gyeongbuk Institute of Science and Technology (DGIST). His research interests include visual surveillance using deep learning and scene understanding for autonomous navigation.

JONG-EUN HA received his B.S. and M.E. degrees in mechanical engineering from Seoul National University, Seoul, South Korea, in 1992 and 1994, respectively, and his Ph.D. in mechanical engineering from KAIST, Daejeon, South Korea, in 2000. From February 2000 to August 2002, he worked at Samsung Corning, developing an algorithm for a machine vision system. From 2002 to 2005, he worked in Multimedia Engineering at Tongmyong University. Since 2005, he has been a professor at the Department of Mechanical and Automotive Engineering, Seoul National University of Science and Technology. His current research interests include deep learning, intelligent robots, and vehicles.